Isofield low-temperature specific heat of single-crystal $Ho_{1-x}Y_xNi_2B_2C$ $(x=0,0.25,0.5,1)$: Probing the magnetocaloric effect in $HoNi_2B_2C$

M. El Massalami
Instituto de Fisica, Universidade Federal do Rio de Janeiro, Caixa Postal 68528, 21945-970 Rio de Janeiro, Brazil

H. Takeya
National Institute for Materials Science, 1-2-1 Sengen, Tsukuba, Ibaraki 305-0047, Japan

C. M. Chaves
Instituto de Fisica, Universidade Federal do Rio de Janeiro, Caixa Postal 68528, 21945-970 Rio de Janeiro, Brazil
(Received 10 November 2003; revised manuscript received 11 March 2004; published 27 July 2004)

Isofield specific heat, $C(T,H)$, of single-crystal $Ho_{1-x}Y_xNi_2B_2C$ ($x=0$, 0.25, 0.5, 1) were measured within the ranges $0.5\ K<T<50\ K$ and $H(\|a)\leqslant 60$ kOe. Linearized spin-wave theory is invoked to analyze the field and temperature dependence of the magnetic specific heat and entropy of $HoNi_2B_2C$ for $T<T_N, H<H_1$ and $T<T_N, H>H_3$. Based on the known low-temperature H-T phase diagram of $HoNi_2B_2C$, this analysis identifies three distinct field regions. (i) The low-field region ($H<H_1$) where the collinear, commensurate $\nearrow\swarrow$ structure is stabilized, and $C_M(T<T_N,H)$ and $S_M(T<T_N,H)$ are well described by the prediction of linearized antiferromagnetic spin-wave analysis. In particular, $(\partial S_M/\partial H)_T>0$, indicating that cooling can be effected by adiabatic magnetization. (ii) The intermediate-field region ($H_1<H<H_3$), where the two metamagnetic states (namely $\nearrow\nearrow\swarrow$ at H_1 and $\nearrow\nearrow\nwarrow$ at H_2) are stabilized. Here no spin-wave analysis is attempted, but it is evident that $(\partial S_M/\partial H)_T>0$ for $H<H_2$ while $(\partial S_M/\partial H)_T<0$ for $H>H_2$. (iii) The high-field region ($H>H_3$) where the saturated $\nearrow\nearrow$ state is being approached. Here, both $C_M(T<T_N,H)$ and $S_M(T<T_N,H)$ follow the description of a ferromagnetic spin-wave analysis; furthermore, $(\partial S/\partial H)_T<0$, indicating that cooling can be effected by adiabatic demagnetization. The magnetocaloric effect above T_N as well as alloying influences on the magnetic properties are discussed.

DOI: 10.1103/PhysRevB.70.014429 PACS number(s): 74.70.Dd, 74.25.Bt, 75.40.Cx, 75.30.Sg

I. INTRODUCTION

Thermodynamical investigations on the tetragonal $HoNi_2B_2C$ revealed rich information about its superconducting and magnetic properties.[1–3] On the one hand, the superconductivity ($T_c\sim 8$ K, $H_{c2}\sim 5$ kOe), as compared to that of the nonmagnetic isomorph YNi_2B_2C ($T_c\sim 16$ K, $H_{c2}\sim 60$ kOe),[4–7] is found to be drastically reduced by multiple magnetic pair-breaking processes.[1,8,9] The magnetism, on the other hand, manifests the following: (i) paramagnetic features that are remarkably anisotropic;[10,11] (ii) a series of spontaneous zero-field magnetic transformations appearing below 8 K:[1,12,13] a spiral state with $\vec{k_c}\simeq 0.92\vec{c}^*$, a modulated state with $\vec{k_a}\simeq 0.585\vec{a}^*$, and later—below $T_N\approx 5$ K—both modulated states are replaced by a commensurate, collinear antiferromagnetic structure; (iii) a cascade of basal-plane field-induced metamagnetic transformations:[3,14,15] as an example, for $H\|a$, a zero-field antiferromagnetic $\nearrow\swarrow$ arrangement is transformed into a $\nearrow\nearrow\swarrow$ state at H_1, later into a $\nearrow\nearrow\nwarrow$ state at H_2, and finally into a paramagnetic saturated $\nearrow\nearrow$ state above H_3 (an arrow represents a ferromagnetically coupled plane along one of the equivalent easy axes $\langle 110\rangle$). These metamagnetic transformations are evident in all of the reported thermodynamical parameters, such as magnetization,[1–3] magnetoresistivity,[2,16,17] and peak intensity of various reflections in the low-temperature, neutron magnetic patterns.[14,15]

In this work, we show that the above-mentioned metamagnetic transformations are evident also in the field-dependent specific heat measurements. In addition, from these specific heat measurements, the character and the type of the elementary magnetic excitations occurring in some of these metamagnetic phases are evaluated. It will be shown that for the lower and higher field limits, the specific heat curves can be described in terms of spin-wave excitations. In fact, the very presence of the plateaus in all the above-cited thermodynamical quantities is a direct manifestation of the fact that, within each of the metamagnetic phases, the density of magnons is very weakly modified by the applied field.

Another advantage of measuring the isofield specific heat is that it allows the complete determination of the magnetocaloric effect and as such gives a clue as to whether such a borocarbide can be used as a working substance in magnetic refrigeration.[18] This possibility is particularly attractive since borocarbides are generally good thermal conductors, with large magnetic entropy, lower ordering temperatures, and a smaller low-temperature lattice specific heat. Furthermore, the reported isofield magnetization[1–3] indicates that its low-temperature $|(\partial M/\partial T)_H|$ is sizable, especially at the neighborhood of T_N. The latter observation, together with the thermodynamic relations

$$(\partial S/\partial H)_T=(\partial M/\partial T)_H \tag{1}$$

and

$$(\partial T/\partial H)_S=-\frac{T}{C_H}(\partial M/\partial T)_H, \tag{2}$$

reinforces the expectation that its magnetocaloric effect is relatively large (M and C_H are the total magnetization and total specific heat of the sample).

This work, with the above-mentioned objectives of investigating the contribution of the elementary magnetic excitations as well as probing the strength of the magnetocaloric effect, report extensive isofield $C(T,H)$ measurements for temperatures down to 0.5 K and for fields up to 60 kOe. For evaluating the nonmagnetic specific heat contribution (within both the superconducting and normal state), we carried out extensive isofield specific heat measurements on YNi_2B_2C for temperatures down to 0.5 K and for fields up to 120 kOe. Finally, the influence of nonmagnetic alloying on the magnetic specific heat, entropy, and magnetocaloric effect were preliminarily investigated in the solid solution $Ho_{1-x}Y_xNi_2B_2C$ ($x=0.25, 0.5$).

II. THEORETICAL EXPRESSION FOR ISOFIELD MAGNETIC SPECIFIC HEAT OF $HoNi_2B_2C$

A. Low-field approximation ($H<H_1$)

At $T<T_N$ and $H<H_1$, the antiferromagnetic $\nearrow\swarrow$ state is maintained.[3,14,19,20] It is then reasonable to assume a Hamiltonian consisting of Zeeman, exchange, and crystal-field interactions (the relatively smaller dipolar, magnetoelastic, and anisotropic exchange terms are ignored),

$$\mathcal{H} = -g\mu_B\vec{H}\cdot\sum_i \vec{S}_i + \sum_{\langle ij\rangle, L\in A,B} \mathcal{J}_{ij}^{L}\vec{S}_i^{L}\cdot\vec{S}_j^{L} + \sum_{\langle ij\rangle A,B} \mathcal{J}_{ij}^{AB}\vec{S}_i^{A}\cdot\vec{S}_j^{B} + g\mu_B\vec{H}_a\cdot\sum_{i\in A}\vec{S}_i^{A} - g\mu_B\vec{H}_a\cdot\sum_{i\in B}\vec{S}_i^{B}. \quad (3)$$

$\vec{S}_i$ is the total angular momentum operator at the ith $4f$ site; the applied magnetic field H is parallel to the anisotropy field H_a; g is the Landé factor, and μ_B is the Bohr magneton. Within the H-T ranges of interest, the magnetic structure of $HoNi_2B_2C$ consists of two sublattices, denoted as A and B (each is a ferromagnetic layer and successive layers are oppositely oriented and stacked along the c axis[12]). $\mathcal{J}_{ij}^{L}$ couples moments $\vec{S}_i^{L}$ to $\vec{S}_j^{L}$ ($L=A$ or B), both are within the same layer (second term); similarly $\mathcal{J}_{ij}^{AB}$ couples similar moments, but each is from a different layer (third term). Finally, the fourth and fifth terms represent the crystalline electric field interaction, the strength of which at very low temperatures and for this two-sublattice model is represented by H_a.[21]

Based on standard small-amplitude spin-wave analysis, the two dispersion modes are

$$\hbar\omega_k^{\pm} = +\sqrt{A^2-B^2} \pm g\mu_B H,$$

$$A = 4\mathcal{J}_o S\left\{1-\frac{1}{2}[\cos(ak_x)+\cos(ak_y)]\right\} + 8\mathcal{J}_1 S + g\mu_B H_a,$$

$$B = 2\mathcal{J}_1 S\left\{\cos\left(\frac{a}{2}k_x+\frac{a}{2}k_y+\frac{c}{2}k_z\right)+\cos\left(\frac{a}{2}k_x+\frac{a}{2}k_y-\frac{c}{2}k_z\right) + \cos\left(\frac{a}{2}k_x-\frac{a}{2}k_y+\frac{c}{2}k_z\right)+\cos\left(-\frac{a}{2}k_x+\frac{a}{2}k_y+\frac{c}{2}k_z\right)\right\}, \quad (4)$$

where $\mathcal{J}_0$ and $\mathcal{J}_1$ represent effectively the exchange couplings among the nearest neighbors within, respectively, the same or neighboring planes. The two distinct field-dependent energy gaps are

$$\Delta^{\pm}(H) = +\sqrt{(g\mu_B H_a)^2 + 16\mathcal{J}_1 g\mu_B S H_a} \pm g\mu_B H = \Delta_0 \pm g\mu_B H. \quad (5)$$

At lower temperature, where the long-wave limit is assumed, the magnon specific heat is

$$C_M(T<T_N, H<H_1) = 3^{3/2}R(\Delta_0/\theta)^3(\Delta_0/2T\pi^2)\sum_{m=1}^{\infty}\{\cosh(m\xi/T)[K_4(m\Delta_0/T) + \langle 1+2\xi^2/\Delta_0^2\rangle K_2(m\Delta_0/T)] - (m\xi/2T)\sinh(m\xi/T) \times[K_4(m\Delta_0/T)-K_0(m\Delta_0/T)]\}, \quad (6)$$

where $K_n(\cdots)$ represents the modified Bessel function of the second kind, $\xi=g\mu_B H/k_B$, and

$$\theta = z|J_{eff}|S = \sqrt[3]{3^{3/2}16\mathcal{J}_1 S^2[8\mathcal{J}_0\mathcal{J}_1 S + 8\mathcal{J}_1^2 S + \mathcal{J}_0 g\mu_B H_a]} \quad (7)$$

is a characteristic temperature, based on which $|J_{eff}|$ can be defined as being an effective exchange interaction that couples a magnetic moment to its z nearest neighbors.

Equation (6) is equivalent to Eq. (25) of Joenk[22] and, moreover, does reproduce our earlier reported zero-field limit.[23] The magnetic entropy in this range of field and temperature is given as

$$S_M(T<T_N, H<H_1) = 3^{1/2}R(\Delta_0/\theta)^3(\Delta_0/2T\pi^2)\sum_{m=1}^{\infty}\{\cosh(m\xi/T) \times[K_4(m\Delta_0/T)-K_2(m\Delta_0/T)] - 3(\xi/2\Delta_0)\sinh(m\xi/T) \times[K_3(m\Delta_0/T)-K_1(m\Delta_0/T)]\}. \quad (8)$$

B. The high-field limit ($H>H_3$)

For $T<5$ K and $H>H_3$, the field-induced saturated $\nearrow\nearrow$ state is approached.[3,14,19,20] Here, the dispersion relation is taken as $\hbar\omega_k=\Delta_F+\alpha_x k_x^2+\alpha_y k_y^2+\alpha_z k_z^2$, where Δ_F is an effective energy gap that reflects the combined influences of exchange, anisotropy, and applied field. $C_M(T,H)$ is then given as[24]

$$C_M(T<5\text{ K},\ H>H_3) = R\left(\frac{T}{4\pi D_F}\right)^{3/2}\sum_{n=1}^{\infty}\exp\left(-\frac{n\Delta_F}{T}\right) \times\left[\frac{15}{4n^{5/2}}+\frac{3\Delta_F}{Tn^{3/2}}+\frac{\Delta_F^2}{T^2n^{1/2}}\right], \quad (9)$$

where D_F is a function of geometrical and exchange factors. The magnetic entropy is then expressed as[24]

$$S_M(T<5\ \mathrm{K},\ H>H_3)=R\left(\frac{T}{4\pi D_F}\right)^{3/2}\sum_{n=1}^{\infty}\exp\left(-\frac{n\Delta_F}{T}\right)\times\left[\frac{5}{2n^{5/2}}+\frac{\Delta_F}{Tn^{3/2}}\right]. \quad (10)$$

III. EXPERIMENT

Single crystal of $Ho_{1-x}Y_xNi_2B_2C$ ($x=0,0.25,0.5,1$) were grown by the floating zone method[25] and were extensively characterized by structural and physical techniques. The isofield total specific heats, $C(T,H)$, were measured on a relaxation-type calorimeter using the Heliox of Oxford Instruments Inc. ($0.5\ \mathrm{K}<T<25\ \mathrm{K}$, $H\leqslant 120$ kOe). The general features of the thermal evolution of $C(T,H)$ are in agreement with the reported field-dependent results of polycrystallines[26] and the zero-field results of single crystals.[23]

For the low-temperature region, $C(T,H)$ of each compound was analyzed as a sum of an electronic C_{el}, a Debye C_D, a nuclear C_N, and a magnetic contribution C_M. It is assumed that C_M is due only to the Ho sublattice and, furthermore, is the only contribution that couples to the applied field (disregarding the weak superconducting contribution). C_N (due only to Ho nuclei) is of dominant importance only at very low temperatures and was evaluated by a least-square fit using the appropriate hyperfine Hamiltonian.[27] C_{el} and C_D for all samples were evaluated from the analysis of the measured specific heat of YNi_2B_2C (not shown): for fields above 60 kOe, the normal state is restored over all of the probed temperature range and $C(T<15\ \mathrm{K},H>60\ \mathrm{kOe})=\gamma_N T+\beta T^3$ where $\gamma_N=(19.5\pm2.0\ \mathrm{K})$ mJ/mol K^2 and $\beta=0.11\pm0.01$ mJ/mol K^4. On the other hand, within the superconducting phase, $C(T<T_c,H=0)=C_S+\beta T^3=3\gamma T^3/T_c^2+\beta T^3=0.26T^3+0.11T^3$ mJ/mol K, in agreement with Refs. 4, 5, and 28. Further, the field-dependent $\gamma(H)$ is given by $[\gamma_N/\sqrt{H_{c2}}]\sqrt{H}$, the same expression as the one reported by Nohara *et al.*[29]

All our isofield measurements were carried out for $H\|a$. For comparing these measurements with the above-mentioned spin-wave theoretical analysis (where $H\|[110]$), we made use of the results of Canfield *et al.*[3] that the moments are confined along the $\langle 110\rangle$ axes and that the influence of the field is only to modify the distribution of the moments along these equivalent axes. Then for identifying the thermal and field evolution within each of these low-temperature metamagnetic states, we carried out the following seven isofield measurements: (i) 0 kOe, 2.5 kOe $<H_1$, scanning the $\nearrow\swarrow$ state; (ii) $H_1<5$ kOe, 10 kOe$<H_2$, scanning the $\nearrow\nearrow\swarrow$ state; (iii) $H_2<20$ kOe, 40 kOe$<H_3$, scanning the $\nearrow\nearrow\nwarrow$ state; and finally (iv) a 60 kOe measurement scanning the $\nearrow\nearrow$ state. According to Fig. 4 of Ref. 3, the latter assumption is reasonable within a 7° misalignment.

IV. RESULTS AND DISCUSSION

A. $Ho_{1-x}Y_xNi_2B_2C$

Zero-field $C_M(T)$ curves of the series $Ho_{1-x}Y_xNi_2B_2C$ ($x=0,0.25,0.5,1$) are shown in Fig. 1. Across the solid solutions, the evolution of T_N with concentration is clearly visible: the Y dilution induces a reduction of T_N. This agrees with the magnetization and resistive results of Eversmann *et al.*[30] In addition, the increase in Y dilution induces a reduction in the height of the peak of $C_M(T=T_N,H=0)$ and an increase in the value of the low-temperature $C_M(T<T_N,H=0)$. It is worth noting that within the $T<T_N$ range, the sum $(C_{el}+C_D)$ of YNi_2B_2C is much less than 1% of the magnetic specific heat of $HoNi_2B_2C$.

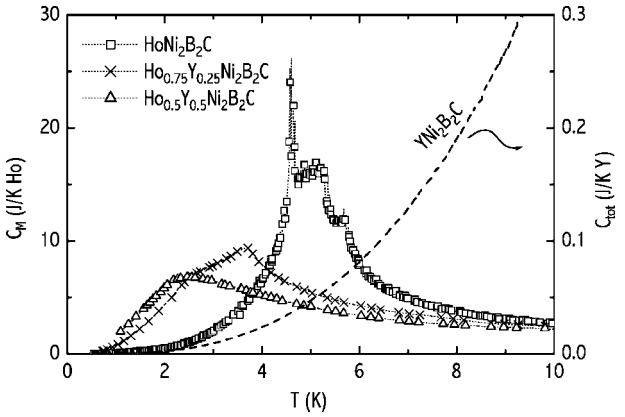

FIG. 1. $C(T,H=0)$ versus T curves of $Ho_{1-x}Y_xNi_2B_2C$ ($x=0,0.25,0.5,1$). $C_M(T,H)$ curves are given for one mole of the Ho atom (left-hand axis) while for YNi_2B_2C, $C_{el}+C_D$ are given for one mole of the Y atom (right-hand axis).

The field dependence of the magnetic specific heat (and entropy) was investigated only for the case of $Ho_{0.75}Y_{0.25}Ni_2B_2C$ in fields up to 20 kOe: as evident from Fig. 2(a), the applied field reduces T_N and the peak height of $C_M(T=T_N,H)$ and suppresses the 2.5 K zero-field shoulder. It is evident also that for $T<5$ K, $(\partial C_M/\partial H)_T<0$; in contrast, for $HoNi_2B_2C$, at similar field conditions, $(\partial C_M/\partial H)_T>0$: such a difference is due to the fact that the random segmentation of some of the magnetic bonds in the Y-doped compound modifies drastically the dispersion relations as compared to those of the parent compound.[31] Figure

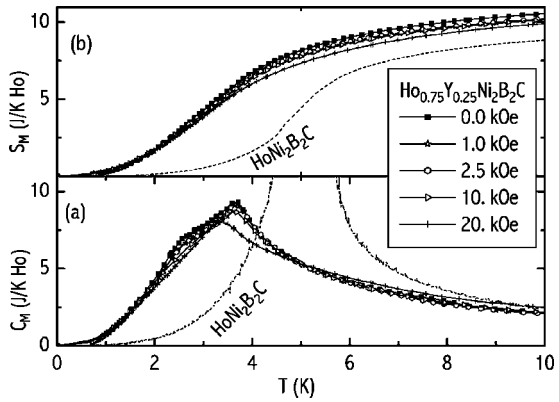

FIG. 2. (a) Isofield $C_M(T,H)$ versus T curves of $Ho_{0.75}Y_{0.25}Ni_2B_2C$. $C_M(T,H)$ curves are given for one mole of the Ho atom. (b) Isofield magnetic entropy of $Ho_{0.75}Y_{0.25}Ni_2B_2C$ as obtained from the numerical integration of $C_M(T,H)/T$. The dashed lines represent the corresponding curves of $HoNi_2B_2C$.

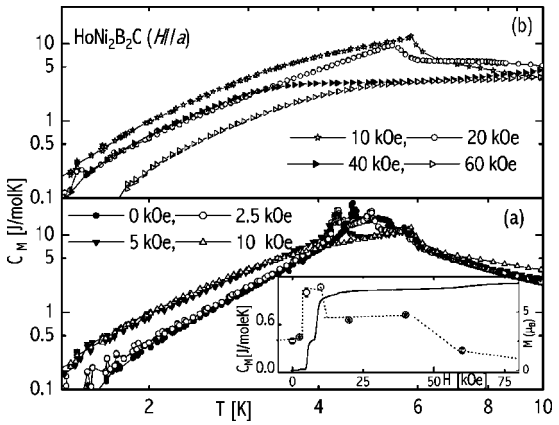

FIG. 3. Isofield $C_M(T,H)$ of $HoNi_2B_2C$. (a) $H=0,2.5,5,10$ kOe. (b) $H=10,20,40,60$ kOe. The inset shows that $C_M(T<T_N,H)$ does mirror the exotic features of the H-T phase diagram as mapped out by, e.g., magnetization measurements: symbols represent $C_M(T=2\ \mathrm{K},H)$ as taken from the main frame (dotted line is a guide to the eye); the solid line represents $M(T=2\ \mathrm{K},H)$ isotherm (H is in the basal plane but 10° away from the a axis. Adapted from Figs. 1 and 4 of Ref. 3).

2(b) shows the isofield magnetic entropy of this sample: evidently, for liquid helium temperatures and for fields up to 20 kOe, the observed change in both S_{mag} and T_{ad} (see below) are very small, indicating that the nonmagnetic alloying of $HoNi_2B_2C$ does not lead to a higher magnetocaloric effect.

B. $HoNi_2B_2C$

Isofield $C_M(T,H\|a)$ curves of $HoNi_2B_2C$ are shown as a linear plot in Fig. 3 while as a $\ln C_M(T,H)$ versus $1/T$ plot in Fig. 4. In the latter figure, the curvature of $\ln C_M(T,H)$ with $H<10$ kOe [Fig. 4(a)] is distinctly different from that with

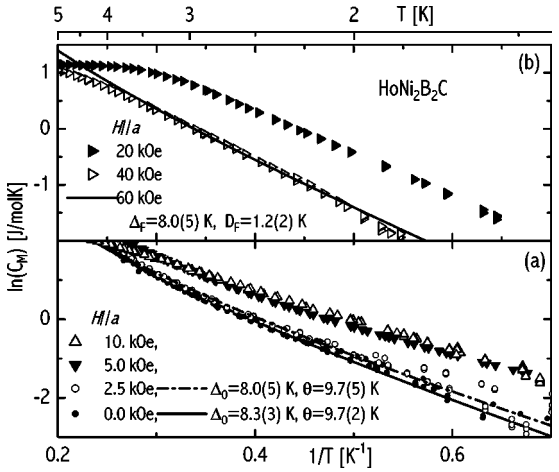

FIG. 4. $\ln[C_M(T,H)]$ versus $1/T$ curves of $HoNi_2B_2C$. (a) $H=0,2.5,5,10$ kOe. The lines on the top of each of the curves with $H=0$, 2.5 kOe are calculations based on Eq. (6) (fit parameters are given in the inset table). (b) $H=20,40,60$ kOe. The line on the top of the $H=60$ kOe curve represents the calculated contribution based on Eq. (9).

$H>10$ kOe [Fig. 4(b)]. These differences, as well as the overall H dependence, can be easily discussed if one recalls that the $H\|a$ phase diagram of $HoNi_2B_2C$ (Refs. 3 and 14) can be subdivided into the above-mentioned three different field regions. Within the low-field limit, no spin-flop process is materialized. Then the linearized spin-wave expression of Eq. (6) can be employed for the analysis of the measured magnetic specific heat. Indeed, as can be seen in Fig. 4(a), the T dependence of $C_M(T,0\ \mathrm{kOe})$ and $C_M(T,2.5\ \mathrm{kOe})$ follows the predictions of Eq. (6) with Δ_0 and θ that are almost field independent [see Fig. 4(a) where Δ_0 and θ are tabulated]. On the other hand, within the high field limit, the moments are driven towards ferromagnetic saturation and here, once more, a linearized spin wave analysis can be employed for the calculation of the magnetic specific heat. Indeed, as can be seen in Fig. 4(b), $C_M(T,60\ \mathrm{kOe})$ compares favorably with the predictions of Eq. (9) with $\Delta_F=8.0(5)$K and $D_F=1.2(2)$K.

For intermediate fields ($H_1<H<H_3$), $HoNi_2B_2C$ develops the above-mentioned succession of field-induced metamagnetic phases. For these phases there are, so far, no analytical expressions that we can use for the analysis of the experimental $C_M(T,H)$ curves. However, for this field range, an insight into the trend of the field dependence of $C_M(T,H)$ can be gained if one recalls the features of the extensively measured $M(T,H)$ curves[1–3] and uses the thermodynamical relation [see Eq. (1)]

$$(\partial C_M/\partial H)_T = T(\partial^2 M/\partial T^2)_H. \tag{11}$$

This assertion is assuringly confirmed in Figs. 3 and 4: on the one hand, since the magnetization curves[1–3] at $H<H_2$ demonstrate that $(\partial^2 M/\partial^2 T)_H>0$, then an increase in H should induce an increase in $C_M(T,H)$; this is confirmed by the results shown in Figs. 3(a) and 4(a) and agrees with the prediction of the field derivative of Eq. (6). On the other hand, since $[\partial^2 M(H>H_2)/\partial^2 T]_H<0$, then an increase in H should induce a decrease in $C_M(T,H)$; this agrees with the results shown in Figs. 3(b) and 4(b) and with the prediction of the field derivative of Eq. (9) where, for this higher field limit $(\partial C_M/\partial H)_T$ is negative.

A comparison of the $C_M(2\ \mathrm{K},H)$ and $M(2\ \mathrm{K},H)$ isotherms (see the inset of Fig. 3) reveals some interesting details. First, for $H<H_1$, both $C_M(2\ \mathrm{K},H)$ and $M(2\ \mathrm{K},H)$ are weakly H dependent, indicating that the density of magnon are weakly field dependent; this is evident in Eq. (5) where the Zeeman energy is only a very small perturbation on the zero-field gap Δ_0. Second, within the intermediate field region, each of $C_M(2\ \mathrm{K},H)$ and $M(2\ \mathrm{K},H)$ manifests steplike jumps at H_1 and H_2 and, after each transition, their values (and the associated density of magnons) are maintained quasi-field-independent (presumably for the same reason as above). It is emphasized that though the density of magnon is very weakly field dependent within each of the metamagnetic states (inset of Fig. 3), however, its temperature dependence is very strong (almost exponential as can be seen in Figs. 3 and 4). Third, for $H>H_3$, $M(2\ \mathrm{K},H)$ is driven towards saturation and, as a consequence, the magnons specific heat is gradually reduced. It is noted that this field evolution

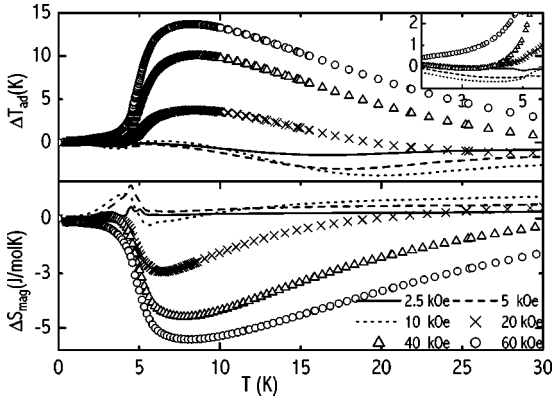

FIG. 5. (a) The thermal evolution of the isothermal change in the magnetic entropy (ΔS_{mag}) of $HoNi_2B_2C$ for the indicated change in the magnetic field. $S_{tot}(T,H)$ is numerically integrated from the corresponding $C_{tot}(T,H)/T$ curve. (b) The thermal evolution of the temperature change (ΔT_{ad}) due to the indicated adiabatic change in the magnetic field. The inset expands the temperature range $2\ \mathrm{K} < T < T_N$.

of $C_M(T,H)$ and $M(T,H)$ isotherms[1–3] is reflected also in the magnetoresistivity[2,16,17] and in the peak intensity of various reflections in the neutron magnetic diffractograms.[14,15] Thus, spin-wave analysis is indispensable for a valid description of low-T thermodynamics of $HoNi_2B_2C$.

From the thermal evolution of the total isofield entropies of $HoNi_2B_2C$, we numerically calculated[18] the magnetic field-induced entropy change $[\Delta S_{mag}(T,\Delta H)_T]$ and the adiabatic temperature change $[\Delta T_{ad}(T,\Delta H)_S]$, shown in Figs. 5(a) and 5(b), respectively. Considering that $HoNi_2B_2C$ is strongly anisotropic[10,11] (hence both ΔS_{mag} and ΔT_{ad}), then cooling can be effected by adiabatic rotation of the single crystal in a strong magnetic field.

Based on Fig. 5, four temperature ranges can be distinguished: (i) the $T < 2$ K range where the applied field is very weak compared to the hyperfine field. As a consequence there is hardly any field dependence in S_{mag} and T_{ad}. (ii) the $2\ \mathrm{K} < T < T_N$ range where the specific heat is dominated by spin-wave excitations. Here, for $H < H_1$, ΔS_{mag} (ΔT_{ad}) increases (decreases) with the applied field in agreement with Eq. (11) and with the intuitive expectation that magnetic disorder in a collinear antiferromagnetic would be increased for an applied field ($< H_{spin\ flop}$) along the easy axis. On the other hand, for $H > H_2$, $\Delta S_{mag}(\Delta T_{ad})$ decreases (increases) with the applied field. For the limit $H > H_3$, this [in agreement with Eq. (10)] suggests that cooling can be obtained by adiabatic demagnetization. (iii) The $T_N < T < 15$ K critical order fluctuating region where there is a large change in both ΔS_{mag} and ΔT_{ad}. As an example, for an adiabatic field changes of 60 kOe at, say, 8 K, ΔT_{ad} amounts to 14 K [see Fig. 5(b)] with a rate of almost 0.23 K per kOe across a temperature span of 10 K. These interesting magnetocaloric features are comparable to the ones observed in some intermetallic magnets,[18] such as $ErAl_2$ or $DyNi_2$. (iv) Finally for higher temperature range, both ΔS_{mag} and ΔT_{ad} are expected to show features that are typical of conventional (anisotropic) paramagnets.

In summary, the measurement and analysis of the isofield $C_M(T,H)$ of $Ho_{1-x}Y_xNi_2B_2C$ ($x=0,0.25,0.5,1$) within the ranges $0.5\ \mathrm{K} < T < 50$ K and $H < 120$ kOe proved to be very helpful for the elucidation of their low-temperature thermodynamics. For $Ho_{1-x}Y_xNi_2B_2C$ ($x=0.25,0.5$), it is shown that magnetic dilution weakens the magnetic couplings, increases the magnetic disorder, shifts the magnetic entropy (as compared to that of $HoNi_2B_2C$) to lower temperatures, and induces a decrease in T_N. For the particular case of $Ho_{0.75}Y_{0.25}Ni_2B_2C$ in fields up to 20 kOe, it is shown that $(\partial S/\partial H)_T < 0$ and that ΔS_{mag} and ΔT_{ad} are smaller than those of the parent compound.

For $HoNi_2B_2C$, at $T < T_N$ and low or high fields, spin-wave analysis was successfully invoked to interpret the field and temperature dependence of the magnetic specific heat: for $H < H_1$, $C_M(T < T_N, H)$ and $S_M(T < T_N, H)$ are well described in terms of linearized field-dependent antiferromagnetic spin-wave excitations and that $\Delta S_{mag} > 0$ while $\Delta T_{ad} < 0$. For $H > H_3$, $C_M(T < T_N, H)$ and $S_M(T < T_N, H)$ follow the description of the ferromagnetic spin-wave analysis and that $\Delta S_{mag} < 0$ while $\Delta T_{ad} > 0$. On the other hand, for $T > T_N$, considerable magnetocaloric effect are manifested: e.g., for an adiabatic field change of 60 kOe at 8 K, ΔS_{mag} reaches almost -6 J/mol K while ΔT_{ad} attains 14 K with a field rate of 0.23 K per kOe. Considering the magnetic and thermal properties of these intermetallic borocarbides, then a higher magnetocaloric effect may be expected.

ACKNOWLEDGMENTS

Partial financial support was provided by Brazilian agencies CNPq and FAPERJ.

[1] P. C. Canfield, B. K. Cho, D. C. Johnston, D. K. Finnemore, and M. F. Hundley, Physica C **230**, 397 (1994).
[2] K. D. Ranthnayaka, D. G. Naugle, B. K. Cho, and P. C. Canfield, Phys. Rev. B **53**, 5688 (1996).
[3] P. C. Canfield, S. L. Bud'ko, B. K. Cho, A. Lacerda, D. Farrell, E. Johnston-Halperin, V. A. Kalatsky, and V. L. Pokrovsky, Phys. Rev. B **55**, 970 (1997).
[4] R. Movshovich, M. F. Hundley, J. D. Thompson, P. C. Canfield, B. K. Cho, and A. V. Chubkov, Physica C **227**, 381 (1994).
[5] H. Michor, T. Holubar, C. Dusek, and G. Hilscher, Phys. Rev. B **52**, 16 165 (1995).
[6] S. V. Shulga, S. L. Drechsler, G. Fuchs, K. H. Muller, K. Winzer, M. Heinecke, and K. Krug, Phys. Rev. Lett. **80**, 1730 (1998).
[7] K. D. Ranthnayaka, A. K. Bhatnagar, A. Parasiris, D. G. Naugle, P. C. Canfield, and B. K. Cho, Phys. Rev. B **55**, 8506 (1997).
[8] H. Eisaki, H. Takagi, R. J. Cava, B. Batlogg, J. J. Krajewski, W. F. Peck, Jr., K. Mizuhashi, J. O. Lee, and S. Uchida, Phys. Rev. B **50**, 647 (1994).
[9] B. K. Cho, P. C. Canfield, and D. C. Johnston, Phys. Rev. Lett. **77**, 163 (1996).

[10] B. Cho, B. N. Harmon, D. C. Johnston, and P. C. Canfield, Phys. Rev. B **53**, 2217 (1996).
[11] U. Gasser, P. Allenspach, J. Mesot, and A. Furrer, Physica C **282-287**, 1327 (1997).
[12] J. W. Lynn, S. Skanthakumar, Q. Huang, S. K. Sinha, Z. Hossain, L. Gupta, R. Nagarajan, and C. Godart, Phys. Rev. B **55**, 6584 (1997).
[13] A. I. Goldman, C. Stassis, P. C. Canfield, J. Zarestky, P. Dervenagas, B. K. Cho, D. C. Johnston, and B. Sternlieb, Phys. Rev. B **50**, 9668 (1994).
[14] A. J. Campbell, D. M. Paul, and G. J. McIntyre, Phys. Rev. B **61**, 5872 (2000).
[15] C. Detlefs, F. Bourdarot, P. Burlet, P. Dervenagas, S. L. Bud'ko, and P. C. Canfield, Phys. Rev. B **61**, R14 916 (2000).
[16] M. El Massalami and E. Baggio-Saitovitch, J. Magn. Magn. Mater. **153**, 97 (1996).
[17] K. Krug, M. Heinecke, and K. Winzer, Physica C **267**, 321 (1996).
[18] V. K. Pecharsky and K. A. Gschneidner, Jr., J. Magn. Magn. Mater. **200**, 44 (1999).
[19] A. Amici and P. Thalmeier, Phys. Rev. B **57**, 10 684 (1998).
[20] V. A. Kalatsky and V. L. Pokrovsky, Phys. Rev. B **57**, 5485 (1998).
[21] C. Kittel, *Quantum Theory of Solids* (Wiley, New York, 1963).
[22] R. J. Joenk, Phys. Rev. **128**, 1634 (1962).
[23] M. El Massalami, R. E. Rapp, F. A. Chaves, H. Takeya, and C. M. Chaves, Phys. Rev. B **67**, 224407 (2003).
[24] L. Walker, in *Magnetism*, edited by G. Rado and H. Suhl (Academic Press, New York, 1963), p. 299.
[25] H. Takeya, T. Hirano, and K. Kadowaki, Physica C **256**, 220 (1996).
[26] J.-H. Choi, H. Doh, E.-M. Choi, H.-J. Kim, S.-I. Lee, T. Yamamoto, T. Kawae, and K. Takeda, J. Phys. Soc. Jpn. **70**, 3037 (2001).
[27] M. Kruis, G. R. Pickett, and M. C. Veuro, Solid State Commun. **14**, 191 (1974).
[28] H. Takeya, S. Miyamoto, K. Yamada, N. Nonose, and K. Kadowaki, Physica C **282-287**, 715 (1997).
[29] M. Nohara, M. Isshiki, H. Takagi, and R. J. Cava, J. Phys. Soc. Jpn. **66**, 1888 (1997).
[30] K. Eversmann, A. Handstein, G. Fuchs, L. Gao, and K. H. Muller, Physica C **266**, 27 (1996).
[31] H. Takeya and M. El Massalami, Phys. Rev. B **69**, 024509 (2004).